PHYSICAL REVIEW B VOLUME 17, NUMBER 1 1 JANUARY 1978

Anisotropic hyperfine interactions in ferromagnetic hcp Co†

D. Fekete, H. Boasson, A. Grayevski, V. Zevin, and N. Kaplan
The Racah Institute of Physics, The Hebrew University of Jerusalem, Israel
(Received 30 November 1976)

The anisotropy of the magnetic hyperfine field H_{hf}, and the angular dependence of the quadrupole splitting ν_q are measured in an NMR study of a fully magnetized single-crystal sphere of ferromagnetic hcp Co. For $\vec{M}$ rotation in a $(\bar{1}\,2\,\bar{1}\,0)$ plane it is found that $H_{hf} = H^0 + H'[(3\cos^2\psi - 1)/2]$, $\nu_q = \nu_q^{rel} + \nu'_q[(3\cos^2\psi - 1)/2]$, where ψ is the angle between $\vec{M}$ and the c axis. The numerical values are $H^0 = -226$ kG, $H' = 5.73$ kG, $\nu_q^{rel} = 24.5$ kHz and $\nu'_q = 196.1$ kHz. A phenomenological interpretation is given and the data are used to examine some aspects of the band model of hcp Co. It is shown that the isotropic part of ν_q, i.e. ν_q^{rel}, can be ascribed to the relativistic contribution of the d band to the electronic-field gradient at the ^{59}Co site. A model in which the orthogonal-plane-wave band calculations concerning the magnetic hyperfine anisotropy can be confronted with the experimental observation is presented.

I. INTRODUCTION

The study of anisotropic distribution of charge and spin densities in ferromagnetic metals is of interest for the understanding of the metallic and magnetic states. Zero-field NMR study of hcp cobalt has been reported some years ago[1] in an attempt to obtain information about the anisotropy of the magnetic hyperfine field and the quadrupole interaction (QI) which reflects the spin and charge distribution in the metal. Recently, the anisotropy in the magnetic hyperfine field was measured by several techniques and contradicting results were reported.[2,3]

A reevaluation of the NMR fast-passage technique used in Ref. 1 reveals the inherent limitations of this technique.[4] In ferromagnets with significantly anisotropic hyperfine fields the fast-passage technique measures the product of the enhancement factor $\eta(\omega)$ and $G(\omega - \omega_0)$, where $G(\omega - \omega_0)$ is the normalized distribution function of local magnetic fields within the wall. This product may be significantly different from the distribution of local fields alone.[4] Secondly, $G(\omega - \omega_0)$ is the total distribution function of the local magnetic fields, including both the distribution of the magnetic hyperfine fields and the dipolar fields, and therefore depends on the unknown variation of the demagnetizing fields H_D within the wall. Thus while at the center of a domain wall the *demagnetizing* field vanishes or at least is very small, as we move away from the center *demagnetizing* fields may be expected to be present, e.g., in the edge of the domain wall $H_d = MD/r$,[5] where r is a measure of the domian size, D is the domain-wall thickness, and M is the magnetization. Comparison of the calculated spectra with Co data in Ref. 1 is rather inconclusive.[4] It is apparent that the only way to remove the above difficulties along with many others is for NMR in ferromagnets to be done on single crystals with an applied field large enough to remove walls from the sample.[4] Using a recently developed technique which enables the observation of NMR in fully magnetized single crystals of ferromagnetic metals, the present paper describes the results of an NMR study in a single crystal of hcp cobalt. The study, which provides accurate measurements of the anisotropy of the magnetic hyperfine field and the angular dependence of the electric field gradients acting on the ^{59}Co nuclei in the sample, enable a reevaluation of the charge and spin distribution in hcp cobalt. The experimental details of the study and the results are presented in Secs. II and III, detailed phenomenlogical interpretation is given in Sec. IV, and Sec. V includes a discussion and conclusions.

II. EXPERIMENTAL DETAILS

Strains, impurities, and other imperfections in real ferromagnets induce microscopic broadening of the NMR line. For an imperfect ellipsoid in an external magnetic field, there exists also a macroscopic broadening caused by the inhomogeneity of the demagnetization field. The elimination, or at least the minimization, of the latter contribution to the line width is a necessary condition for the observation of NMR signals in a full magnetized single crystal. Criteria for the observability of narrow NMR in metallic single-crystal ferromagnets were discussed recently.[6] According to these criteria, both the deviation from sphericity δ and the surface roughness of a spherical sample play a role in the macroscopic inhomogeneous line broadening. Therefore, we shall outline here the method used in preparing the cobalt for the NMR observations.

The single crystal of hcp cobalt was grown by zone-melting a 0.9999% pure cobalt rod in an electron beam furnace. A sphere with a diameter of ~0.5 cm was cut from the rod by spark erosion.

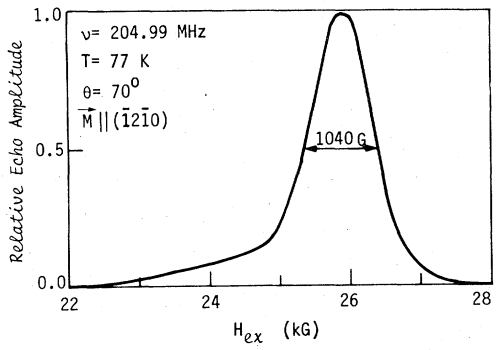

FIG. 1. ^{59}Co NMR absorption profile in a wall free ferromagnetic sphere of hcp cobalt.

The sphere was then ground and polished mechanically with Al_2O_3 powder and etched in a solution of one part H_2O_2 (10%) and four parts HCl. The polishing process and the shape of the specimen were checked periodically with an optical goniometer. When the polishing process removed the strained material, the etching solution attacked preferentially the $(\bar{1}1\bar{2}0)$ planes,[7] and a sixfold visual reflection pattern developed with intersecting centers coinciding with the c-axis poles on the sphere. When most of the strained material was removed, the sphere was held magnetically at the end of a rotating electrode and electropolished[8] in a solution of 68% N,N-dimethylformamide, 29% $CoCl_2 \cdot 6H_2O$, and 3% H_2O, all in wt.%. The stainless-steel container holding the electrolyte served as the second electrode, and the voltage between the electrodes was maintained around 22 v. Finally the crystal was annealed under H_2 atmosphere at 300 °C for 20 h. X-ray Laue photography analysis following each step indicated that all of the above steps were indeed necessary to minimize structural damage at the surface of the sphere, an important point if the measurement is to be performed in a well-defined hcp phase.

Final checks of the sample revealed fractional deviation from sphericity $\delta/d = \pm 0.002$ were d is the diameter of the sphere. It is somewhat more difficult to estimate the surface roughness δ'. The abrasive powder used in the final stages was 0.3 μm but the subsequent electropolishing process may have changed the roughness drastically. Based on observation with a regular microscope we estimate very crudely $\delta' \simeq 1$ μm. For the quoted values of δ/d and δ', the criterion mentioned above[6] predicts a lower limit for the shape induced inhomogeneous broadening, $\Delta H \simeq 1$kG.

The sphere was wrapped in a 10-μm-thick Mylar foil and placed in a few turns of tightly wound copper wire (AWG No. 46) which formed part of the tank circuit of a conventional spin-echo spectrometer. The sphere was mounted so that an external magnetic field H_{ex} could rotate $\vec{M}$ within the sphere in a $(\bar{1}1\bar{2}0)$ plane. Saturation of M was ensured by using H_{ex} in the 15–30 kG range as compared with the demagnetization field $H_d = \frac{4}{3}\pi m \simeq 6$ kG for a sphere of Co. The NMR absorption profiles were scanned through, at a fixed radio frequency and given $\vec{H}_{ex}$ direction, by recording the spin-echo amplitude following a $\frac{1}{2}\pi - \pi$ rf sequence as function of $|H_{ex}|$ (see Fig. 1). In addition, for $\vec{H}_{ex}$ value corresponding to the maxima, we have recorded accurately, with a digital signal averaging system, the modulated echo-decay envelope as a function of the separation τ between the rf pulses (see Fig. 2). All of the measurements reported here were made at 4.2 77, and 295 K.

III. RESULTS AND DATA ANALYSIS

The coupling of the ^{19}Co nucleus with the environment can be described by an interaction Hamiltonian, including both Zeeman and quadrupole interaction, of the form

$$\mathcal{H}_{hf} = \gamma\hbar H I_\xi + \frac{e^2 Q q_\xi}{4I(2I-1)}\left[3I_\xi^2 - I(I+1)\right], \qquad (1)$$

where Q is the nuclear quadrupole moment and γ is the nuclear gyromagnetic ratio. The ξ axis is chosen in the direction of the total magnetic field $\vec{H} = \vec{H}_{hf} + \vec{H}_{ex}$ acting on the nucleus, $\vec{H}$ is the sum of the hyperfine field $\vec{H}_{hf}$ and the external field $\vec{H}_{ex}$, eq_ξ is the component of the electric field gradient (EFG) tensor in the direction of $\vec{H}$. The resonance frequency corresponding to the $(m \leftrightarrow m+1)$ transition is given by

$$\nu_{res} = \nu_L + \nu_q(m - \tfrac{1}{2}), \qquad (2)$$

where only the first order of the e^2qQ term is considered, with $\nu_L = \gamma|H|/2\pi$ and $\nu_q = 3e^2Qq_\xi/2I(2I-1)h$ using the notations of Ref. 9. Actually the quadrupole splitting in the present system is too

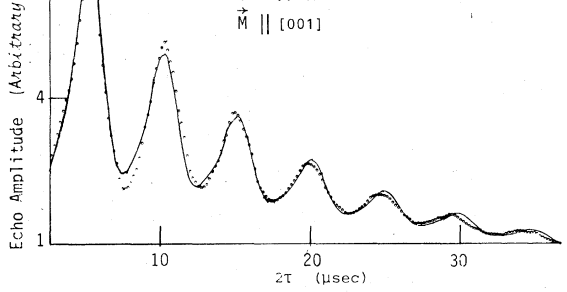

FIG. 2. Spin-echo decay modulations at 77 K. Points represent experimental values and the solid curve is calculated by the model.

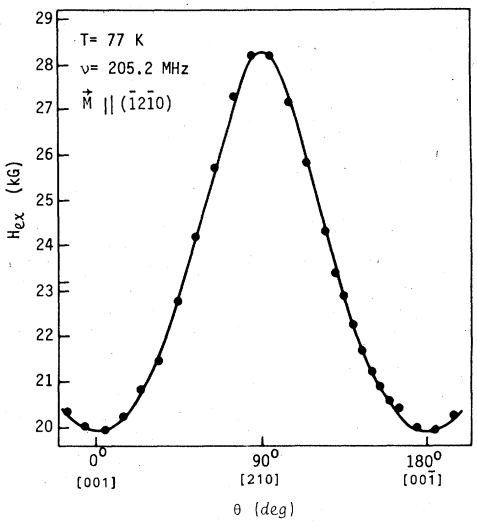

FIG. 3. Angular dependence of H_{ex} values corresponding to the NMR absorption maxima. θ is the angle between $\vec{H}_{ex}$ and [001] in the $(\bar{1}2\bar{1}0)$ plane.

small to be observed directly, and only an unsplit line is observed whose width depends on the direction of $\vec{M}$ because of the quadrupolar broadening. A typical line profile for the particular $\vec{M}$ direction where ν_q vanishes is shown in Fig. 1 with a width of about 1 kG. The frequency of the center of the line is given by ν_L, the first term in Eq. (2). Figure 3 displays (black points) $|H_{ex}|$ values corresponding to a constant ν_{res} as a function of the angle θ between H_{ex} and the c axis in the $(\bar{1}2\bar{1}0)$ plane.

In cobalt, $\vec{H}_{hf}$ is parallel and opposite to the $\vec{M}$ direction so that by varying $\vec{M}$ we can actually measure $\vec{H}_{hf}$ in different orientations. However, because of the magnetic anisotropy, $\vec{M}$ is *not* collinear with the external field $\vec{H}_{ex}$ except when $\theta = 0°$ and $\theta = 90°$. The direction of $\vec{M}$ and hence the direction of $\vec{H}_{hf}$ is obtained from the equilibrium condition between the torque exerted by $\vec{H}_{ex}$ and the torque produced by the magnetic anisotropy, given by

$$-\frac{\partial E_c}{\partial \psi} = -\vec{H}_{ex} \times \vec{M}\,, \tag{3}$$

where ψ is the angle between $\vec{M}$ and the c axis and E_c is the free energy of the crystalline magnetic anisotropy, given by

$$E_c = K_2 \sin^2\psi + K_4 \sin^4\psi\,. \tag{4}$$

From Eqs. (3) and (4) we obtain

$$H_{ex} M \sin(\theta - \psi) = (K_2 + K_4)\sin 2\psi - \tfrac{1}{2}K4 \sin 4\psi\,, \tag{5}$$

where K_2, K_4, and $\vec{M}$ are given as function of the temperature in Ref. 7. The values of H_{ex} and θ are experimental values as mentioned above. Using Eq. (2) we find

$$H_{hf} = -H_{ex}\cos(\theta - \psi) - [-H_{ex}^2 \sin^2(\theta - \psi) + (2\pi\nu_L/\gamma)^2]^{1/2}\,. \tag{6}$$

Figure 4 displays (black points) H_{hf} values [Eq. (5)] as a function of $\vec{M}$ direction, calculated from Eq. (5) for two different temperatures.

The second term in Eq. (2), the nuclear quadrupolar interaction, was measured by utilizing spin-echo technique first reported by Abe *et al.*[10] The method can be outlined briefly as follows: When a quadrupolar interaction (QI) term is added to a nuclear Zeeman Hamiltonian, the usual monotonic T_2 decay of the nuclear spin-echo envelope following a $\frac{1}{2}\pi - \tau - \pi$ pulse sequence is modulated by oscillation, the frequency of which depends on the QI. For an axially symmetric efg and $I(^{59}\mathrm{Co}) = \frac{7}{2}$, the explicit expression given in Ref. 10 for the modulation amplitude is

$$m(2\tau) = \sum_{n=0}^{6} C_n \cos(2n\nu_q\tau + \delta_n)\,, \tag{7}$$

where C_n and δ_n are constants depending on initial conditions and on the shape and width of the rf pulses. It has been found in the course of the present study that for practical purposes only the first and the second harmonic terms are needed for best fitting Eq. (7) to the experimental results. In

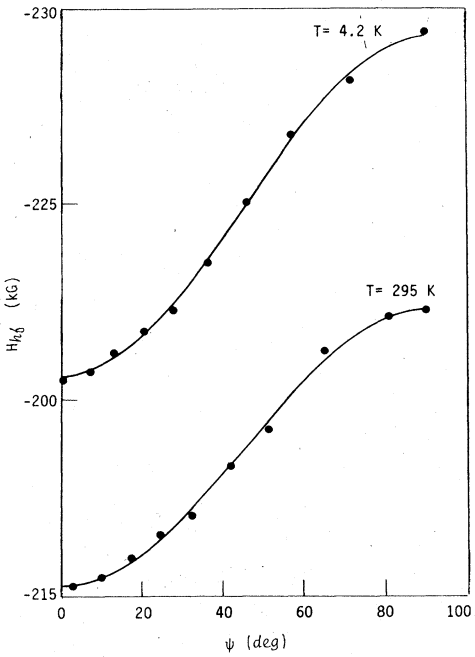

FIG. 4. Angular dependence of H_{hf} values (points) at 4.2 and 295 K. ψ is the angle between $\vec{M}$ and [001] in the $(\bar{1}2\bar{1}0)$ plane. The solid curves were calculated by the model.

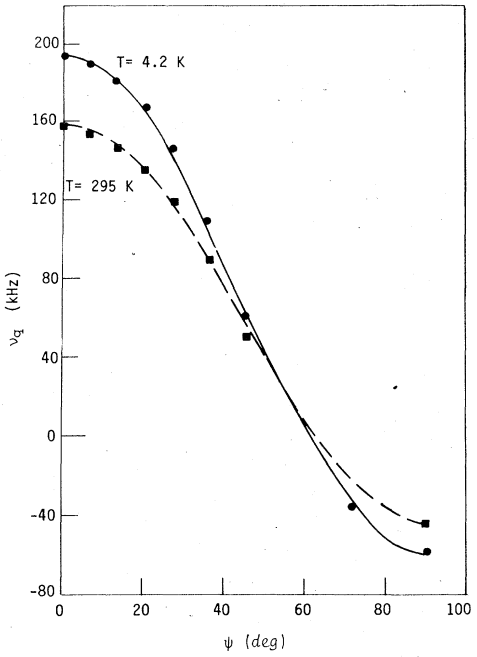

FIG. 5. Angular dependence of ν_q values (circles measured at 4.2 K, squares measured at 295 K). ψ is the angle between $\vec{M}$ and [001] in the $(\bar{1}2\bar{1}0)$ plane. The solid curves were calculated by the model.

a real ferromagnet, in addition to the transverse T_2 decay, there exists a decay of the modulation due to the inhomogeneous broadening of the QI. This broadening causes dephasing of the modulation and can be approximately described by an additional exponential decay time T_2'. We thus write for the echo amplitude at $t = 2\tau$:

$$E(2\tau) = \exp(-2\tau/T_2) \times \{1 + [C_1 \cos(2\nu_q\tau + \delta_1) + C_2 \cos(4\nu_q\tau + \delta_2)] \exp(-2\tau/T_2')\}, \quad (8)$$

with T_2, T_2', C_1, C_2, δ_1, δ_2, and ν_q as parameters. The experimental modulated echo-decay envelope (black points) is shown in Fig. 2 as a function of the separation τ between the rf pulses at 77 K. A least-square fitting of the theoretical functional decay [Eq. (8)] to the experimentally recorded data (solid line in Fig. 2) yields ν_q values with typical accuracy of ±0.6%. The technique also enabled us to find the macroscopic broadening of the QI and it was found that $T_2' = 40$ μsec corresponding to a QI broadening of ~2.5 G. A similar procedure was used for various $\vec{H}_{ex}$ orientation, and Fig. 5 displays (points) the observed ν_q values as a function of the direction of $\vec{M}$ in the $(\bar{1}2\bar{1}0)$ plane for two different temperatures.

IV. INTERPRETATION

A. Magnetic hyperfine field (H_{hf})

The hexagonal structure of the present system dictates $\vec{H}_{hf}$ of the form

$$(H_{hf})_\xi = H^0 + H'(\tfrac{3}{2}\cos^2\psi - 1). \quad (9)$$

The above anisotropy arises mainly from two contributions: first, the spin dipolar field $\vec{H}_d$ due to the spin moment of the $3d$ electrons, a field which reflects the spin distribution around the nucleus, and second the field $\vec{H}_L$ caused by the unquenched part of the orbital moment of the $3d$ electrons. A model calculation of the spin dipolar contribution and its angular dependence yields[11]

$$(H_d)_\xi = \mu_B n_h \langle 3\cos^2\theta - 1\rangle \langle r_{3d}^{-3}\rangle \left(\frac{3\cos^2\psi - 1}{2}\right) \equiv H_d' \left(\frac{3\cos^2\psi - 1}{2}\right), \quad (10)$$

where μ_B is the Bohr magneton and n_h is the number of holes in the d band, assumed to be 1.7 for metallic Co. The orbital field H_L is given by[11]

$$(H_L)_\xi = -2\mu_B \langle L_\xi\rangle \langle r_{3d}^{-3}\rangle = H_L^0 + H_L'(\tfrac{3}{2}\cos^2\psi - 1), \quad (11)$$

where

$$H_L^0 = -\tfrac{2}{3}\mu_B \langle r_{3d}^{-3}\rangle (\langle L_\parallel\rangle + 2\langle L_\perp\rangle) = -2\mu_B \langle r_{3d}^{-3}\rangle \langle L\rangle^0,$$

$$H_L' = -\tfrac{4}{3}\mu_B \langle r_{3d}^{-3}\rangle (\langle L_\parallel\rangle - \langle L_\perp\rangle) = -2\mu_B \langle r_{3d}^{-3}\rangle \langle L\rangle',$$

and the subscripts $\parallel$ and $\perp$ are referred to the crystalline c axis. Thus $(H_L)_\xi$ is separated into an isotropic term and an angular-dependent term with a functional dependence that is identical to that of Eq. (9). Using the definition of the spectroscopic splitting factor

$$\langle L_\parallel\rangle = (g_\parallel - 2)\langle s\rangle; \quad \langle L_\perp\rangle = (g_\perp - 2)\langle s\rangle, \quad (12)$$

and the relation $\langle s\rangle = -\tfrac{1}{2}n_h$, Eq. (11) can be written also as

$$(H_L)_\xi = \tfrac{1}{3}\mu_B n_h \langle r_{3d}^{-3}\rangle (g_\parallel + 2g_\perp - 6) + \tfrac{2}{3}\mu_B n_h \langle r_{3d}^{-3}\rangle (g_\parallel - g_\perp)[(3\cos^2\psi - 1)/2]. \quad (13)$$

The values of H^0 and H' were determined phenomenologically in the present study by best fitting (solid line in Fig. 4) Eq. (9) to the derived values of H_{hf}, obtained from Eq. (6). At 4.2 K, we find $H^0 = 226.0 \pm 0.1$ kG and $H' = 5.726 \pm 0.1$ kG. Values corresponding to other temperatures are given in Table I.

The above experimental results can be examined critically in two ways. First, one can substitute in the theoretical expressions [Eqs. (10) and (13)] independent results obtained by other techniques, and thus examine the validity of the present interpretation. Secondly, the anisotropic part H' of

TABLE I. H^0 and H' values at different temperatures.

T (K)	H^0 (kG)	H' (kG)
4.2	-226.0 ± 0.1	5.73 ± 0.1
77	-225.7 ± 0.1	5.60 ± 0.1
295	-219.9 ± 0.1	4.63 ± 0.1

$H_{\rm hf}$ can be used to examine some aspects of the band model. The following experimental values are used: (i) $\langle 3\cos^2\theta - 1\rangle = 0.0023$, obtained from neutron diffraction experiments[11,12]; (ii) $g_{\parallel} = 2.17$, obtained from ferromagnetic resonance[13]; (iii) assuming the anisotropy in M stems from orbital contribution only, high-field susceptibility measurements[14] yield

$$\frac{g_{\parallel} - g_{\perp}}{g_{\parallel}} = \frac{M_{\parallel} - M_{\perp}}{M_{\parallel}} = 450 \times 10^{-5} \text{ at } 4.2 \text{ K}. \qquad (14)$$

Finally we use $\langle r_{3d}^{-3}\rangle = 6.0354$ a.u., computed for Co^{+2}.[15] Substituting the above values in Eqs. (10) and (13) we obtain the combined anisotropy of the spin-dipolar and orbital fields, $H'_d + H'_L = H' = 5.659$ kG. This result, which is in excellent agreement with the experimental value derived in the present study for 4.2 K, confirms the validity of our interpretation and encourages us to outline in the next section an attempt for a comparison between our experimental results (Table I) and the prediction of a proper band-structure model calculation.

B. Electric field gradient (efg)

The efg at a nucleus arises from the distribution of the charge about it and is given by $e\int [\rho(r)/r_3] \times (3\cos^2\theta - 1)\, dv$. For convenience it is useful to consider a field gradient at the site of a given nucleus in a metal as arising from several separate sources. The contribution due to the surrounding nearby point charges at the hcp lattice sites together with a uniform compensating electron charge, is given by[16]

$$q_{\rm latt} = Z[\,0.0065 + 4.3584(1.633 - c/a)\,]/a^3\,, \qquad (15)$$

where Z is the ionic charge and c and a are the hexagonal lattice constants. The deviation of the conduction-electron charge from uniform density must also be included in the lattice contribution. This contribution due to conduction electrons outside the central atomic spehere can be expressed as an extra screening term[17] in Eq. (15) or alternatively by changing the outside ionic charges to an effective-ion charge[18] $Z' = \beta Z$. Both the conduction electrons within the atomic sphere and the central closed-shell core electrons enhance the lattice contribution to the efg, the enhancement factor being $-\gamma_\infty$ for the core electrons[19] and γ_{ce} for the conduction electrons.[20] Thus, the overall lattice contribution to q [Eq. (1)] in an hcp lattice is given by

$$(q_{\rm latt})_\zeta = \beta(1 - \gamma_\infty + \gamma_{ce}) q_{\rm latt}[(3\cos^2\theta - 1)/2]\,. \qquad (16)$$

Next, consider efg contributions intrinsic to the ion. Within the central atomic sphere there is a contribution due to the $3d$ valence electrons. However, the crystal field in hcp cobalt splits the $3d$ electron states into the three substates A_{1g}, E_{1g}, E_{2g}, and the mixing of the different symmetry states is close to the statistical 20%-40%-40% admixture characteristic of a spherical distribution.[21] Thus it is expected that the "normal" efg due to the $3d$ electrons will be rather small. Now it has already been demonstrated previously that significant relativistic QI (RQI) is present even for spherical S-state ions such as Eu^{2+} and Mn^{2+}.[22-24] The RQI is usually ignored in non-S states in which the "normal" QI is large, but as a result of the nearly spherical charge distribution[21] mentioned above, the RQI becomes significant in the present case of hcp Co even though it is not an S-state metal. To see the physical origin of the RQI we note that in the relativistic description of the atoms, the radii of electrons in the same shell are no longer equal, contrary to the situation in the nonrelativistic description.[24]

Using the notation of Refs. 23 and 25 the band-model prediction for the isotropic part of the relativistic efg [Eq. (29) of Ref. 26] is

$$(q_{\rm rel})_\zeta = -\frac{2}{5}\frac{\lambda}{(2l+1)^2}\,[-(l+2)R_{++} + 3R_{+-} + (l-1)R_{--}] \times \Bigg(\sum_{E_n < E_{F\,\rm maj}} {\sum_{m\neq n}}' \frac{2A_{nm}^2}{E_n - E_m} + \sum_{E_n < E_{F\,\rm min}} \sum_{m\neq n} \frac{2A_{nm}^2}{(E_n - E_m)} - \sum_{E_n < E_{F\,\rm maj}} {\sum_{m\neq n}}' \frac{B_{nm}^2 + C_{nm}^2}{E_n - E_m - 2\epsilon} - \sum_{E_m < E_{F\,\rm min}} \sum_{m\neq n} \frac{B_{nm}^2 + C_{nm}^2}{E_n - E_n - 2\epsilon} \Bigg), \qquad (17)$$

and it has been shown[26] that the angular dependence of $(q_{\rm rel})_\zeta$ is negligible in hcp Co. Numerical evaluation of Eq. (17) requires a detailed knowledge of the band-structure parameters A_{mn}, B_{mn}, and C_{mn}. In the absence of such knowledge, we can still use the approximation [Eq. (32) in Ref. 26],

$$(q_{\mathrm{rel}})_\zeta = -\tfrac{8}{5}\,[\epsilon/\Delta(2l+1)^2] \times[-(l+2)R_{++}+3R_{+-}+(l-1)R_{--}]\langle L_\zeta\rangle\,, \tag{17a}$$

where 2ϵ is the exchange splitting between spin-up and spin-down d electrons and Δ is the mean level separation in the bands. Thus the total efg according to Eqs. (16) and (17) is given by

$$q_\zeta = (q_{\mathrm{rel}})_\zeta + \beta(1-\gamma_\infty+\gamma_{ce})q_{\mathrm{latt}}\,(\tfrac{3}{2}\cos^2\psi - 1)\,. \tag{18}$$

Very recently, a surprisingly simple relation has been observed phenomenologically between the point-charge model prediction for the efg and the efg in the corresponding metallic solids.[27] According to this relation, the total efg is given by

$$q_\zeta = (q_{\mathrm{rel}})_\zeta + (1-K)_\beta\,(1-\gamma_\infty)q_{\mathrm{latt}}\,[(3\cos^2\psi - 1)/2]\,, \tag{19}$$

where $K=+3, \beta=1$.[27] With the help of Eqs. (2), (18), and (19) we can now delineate ν_q into an isotropic term and an angular-dependent term,

$$\nu_q = \nu_q^{\mathrm{rel}} + \nu_q'\,(3\cos^2\psi - 1)/2\,, \tag{20}$$

where ν_q^{rel} and ν_q' are calculable either by Eq. (18) or Eq. (19) after multiplying the appropriate efg by the coefficient of Eq. (2).

In the following, we shall assume that the isotropic quadrupole term observed experimentally is indeed caused by the relativistic correction discussed above. With this assumption, measurements of the angular dependence and the c/a dependence of the nuclear quadrupole frequency ν_q permit the determination of the different contributions to the efg. To begin with, we can separate the experimental relativistic contribution from all other contributions because the first is isotropic whereas all others have a $(3\cos^2\psi - 1)/2$ dependence of $\vec{M}$. A best fitting of Eq. (20) (solid and dashed lines in Fig. 5) to the experimental points yield the value of ν_q^{rel} and ν_q' at various temperatures (see also Table II). At 4.2 K

$$\nu_q^{\mathrm{rel}} = 24.4 \pm 0.5 \text{ kHz, and } \nu_q' = 169.1 \pm 0.5 \text{ kHz}\,.$$

Next, ν_q' itself, assumed in our model [Eqs. (15), (16), (19), (20)] to be proportional to q_{latt} and $(q_{\mathrm{latt}})_\zeta$, can be examined rather critically by measuring ν_q' as a function of the ratio c/a in hcp cobalt. To see this, note that the particular value of

TABLE II. ν_q^{rel} and ν_q' values at different temperatures.

T (K)	ν_q^{rel} (kHz)	ν_q' (kHz)
4.2	24.4 ± 0.5	169.1 ± 0.5
77	24.7 ± 0.5	164.8 ± 0.5
295	22.8 ± 0.5	134.8 ± 0.5

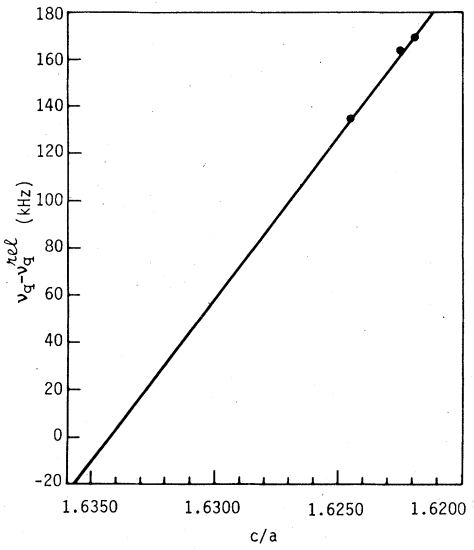

FIG. 6. Plot of $\nu_q - \nu_q^{\mathrm{rel}}$, for $\vec{M}$ along the c axis, as function of c/a. Temperature is the implicit parameter. The solid curve is a linear best fit to the data points.

c/a for which q_{latt} [Eq. (15)] happened to vanish is not a property of the hexagonal symmetry in itself but rather a result of the physical model constructed to derive Eq. (15). Thus contributions to ν_q' from other sources not considered in the original derivation, will not necessarily vanish when q_{latt} of Eq. (15) vanishes.[28] Our experimental results are shown in Fig. 6, where $\nu_q - \nu_q^{\mathrm{rel}}$ at $\theta=\psi=0°$, i.e., ν_q', is shown as a function of c/a (points), with the temperature as the implicit parameter. The temperature dependence of c/a was taken from Ref. 29. A nearly linear temperature and c/a dependence of ν_q is verified,[1] and extrapolation of the linear best fit of ν_q' (solid line in Fig. 6) yields a small residual ν_q' value, -8 ± 12 kHz, for $c/a = 1.63449$ where q_{latt} should have vanished according to Eq. (15). At this stage a remark is called for concerning the sign of the various measured ν_q's. In the present NMR study, the absolute sign of the efg cannot be determined and thus so far we can only assert that ν_q' and ν_q^{rel} are of the same sign, and the possible residual ν_q' discussed above is of an opposite sign to the other two. This residual value, if real, could reflect a contribution due to hexagonal distortions of the $3d$ and conduction electrons of the central ion, induced by covalency and/or other lattice-originated hexagonal crystal-field effects not included in Eq. (15). Within the limit of accuracy of the present study, however, the above results indicate that the possible lattice contribution to aspherical distribution of the charges within each ionic core is negligible and it is thus concluded that indeed

ν_q' originates solely from lattice contributions.

For further examination of our interpretation we shall calculate ν_q' and $\nu_q^{\rm rel}$ according to Eqs. (18), (19), and (20) and compare the results with the experimental data.

$\nu_q^{\rm rel}$: Substituting in Eq. (17a) the value $\langle L_\xi \rangle = 0.14$ obtained from Eq. (12) and Ref. 14, $[-(l+2)R_{++} + 3R_{+-} + (l-1)R_{--}] = 0.1328$ a.u. appropriate for Co^{+2},[23,30] for which the effective nuclear charge is $Z_{\rm eff} = 27 - 10 + 2 = 19$, and assuming $\epsilon/\Delta \simeq 1$, we obtain $\nu_q^{\rm rel} = -10.3$ kHz. This is a very crude estimate since the approximation in Eq. (17) is valid only for $\epsilon/\Delta < 1$ while $\epsilon/\Delta \simeq 1$ is more realistic.

ν': Substituting [in Eqs. (15), (18), (19), and (20)] $Z = 2$,[18] $\gamma_\infty = 9.14$ computed for Fe,[21] $c/a = 1.621907$ appropriate to 4.2 K,[29] and assuming $\beta = 1$, we fine either $\nu_q' = 88.2$ kHz. [from Eq. (18)], or $\nu_q' = 176.4$ kHz [from Eq. (19)].

V. DISCUSSION AND CONCLUSIONS

(i) $H_{\rm hf}$: We shall confine the present discussion to the $\langle L_\xi \rangle$ part of the angular-dependent term as theoretical value of $\langle L_\xi \rangle$ can be separated into an isotropic term and an angular dependent term as done in Eq. (11). With notations from Ref. 25 and 26 one obtains

$$\langle L_\xi \rangle = -\frac{\lambda}{3}\left(\sum_{E_n < E_{F\,\rm maj}} \sum_{m\neq n}{}' \frac{A_{nm}^2 + B_{nm}^2 + C_{nm}^2}{E_n - E_m} - \sum_{E_n < E_{F\,\rm min}} \sum_{m\neq n}{}' \frac{A_{nm}^2 + B_{nm}^2 + C_{nm}^2}{E_n - E_m} \right)$$

$$-\frac{\lambda}{3}\left(\sum_{E_n < E_{F\,\rm maj}} \sum_{m\neq n} \frac{2A_{nm}^2 - B_{nm}^2 - C_{nm}^2}{E_n - E_m} - \sum_{E_n < E_{F\,\rm min}} \sum_{m\neq n}{}' \frac{2A_{nm}^2 - B_{nm}^2 - C_{nm}^2}{E_n - E_m} \right) \frac{3\cos^2\psi - 1}{2}$$

$$\equiv \langle L^0 \rangle_{\rm band} + \langle L' \rangle_{\rm band} \left(\tfrac{3}{2}\cos^2\psi - 1\right). \qquad (21)$$

The form of $\langle L_\xi \rangle$ in Eq. (21) illustrates vividly the critical manner by which accurate measurements of the microscopic quantity $H_{\rm hf}$ can test basic predictions of the band-model calculations. The functional form of $\langle L_\xi \rangle$ [Eq. (21)] can be confronted with the experimental angular dependence of $(H_L)_\xi$, regardless of the particular value chosen for the spin-orbit interaction parameter λ. The theoretical ratio $\langle L' \rangle_{\rm band}/\langle L^0 \rangle_{\rm band}$ is independent of λ and should depend only on the band predictions. The experimental ratio H_L'/H_L^0 depends only on the experimental value of $\langle L \rangle'/\langle L \rangle^0$ [Eq. (11)]. Once there is an agreement between the computed and the experimental values of $\langle L \rangle'/\langle L \rangle^0$ we can find directly the exact value of λ appropriate to the band situation in hcp cobalt. Thus one may use the above procedure to clarify the discrepancies between observed and band-computed g value.[25]

(ii) efg: Comparing the experimental and calculated values of the preceding section we find that both Eqs. (18) and (19) require $\nu_q^{\rm rel}$ and ν_q' of a similar sign, i.e., negative, but only Eq. (19) yields proach [i.e., Eq. (19)) is further supported by the fact that the measured efg, $q = (-1.8 \pm 0.2) \times 10^{23}$ cm^{-3},[11] acting on Fe impurities in hcp cobalt is almost the same as the efg, $q = -1.6 \times 10^{23}$ cm^{-3}, acting on cobalt ion in hcp cobalt, in agreement with the assumption[27] that the extraionic gradient should be universally correlated to $q_{\rm latt}(1-\gamma_\infty)$ which is the same for both ions.[27]

The agreement between the computed and the experimental values of $\nu_q^{\rm rel}$ is poor, but this is perhaps not surprising considering the crudeness of the approximation used. For example, in the derivation of $\nu_q^{\rm rel}$ in Sec. IV we have neglected possible "quadrupolarization" of conduction electrons[27,31] induced by the RQI [Eq. (17)] as well as a shielding factor R,[19] both of which might affect the numerical value of $\nu_q^{\rm rel}$. However, whatever the magnitude of $\nu_q^{\rm rel}$, we assume that at least the sign of $\nu_q^{\rm rel}$ is negative as computed. The present study provides an experimental confirmation that both the magnitude and the sign of ν_q' are correctly predicted by the model calculation [Eq. (19)].

Combining the results of the present detailed directional hyperfine study with the results of a very recent publication[32] concerning the high-field Knight shift in single-crystal cobalt, we may conclude that NMR measurements in single-domain single-crystal samples of ferromagnetic metals indeed provide novel and valuable information concerning the electronic structure of such systems.

*Supported in part by the U.S.–Israel Binational Science Foundation.

[1]M. Kawakami, T. Hihara, Y. Koi, and T. Wakiyama, J. Phys. Soc. Jpn. 33, 1591 (1972).

[2]S. G. Bailey, D. C. Creagh, and G. V. H. Wilson, Phys. Lett. A 44, 229 (1973).

[3]P. C. Lanchester, N. F. Whitehead, and P. Wells, J. Phys. F 5, 247 (1975).

[4]M. A. Butler, Phys. Rev. 8, 5122 (1973).
[5]M. Weger, Ph.D. thesis (unpublished).
[6]D. Fekete, A. Grayevskey, N. Kaplan, and E. Walker, Solid State Commun. 17, 537 (1975).
[7]W. Sucksmith, J. E. Thompson, Proc. R. Soc. A 225, 362 (1954).
[8]A. Turashov, T. Mukhammetgaliev, and R. Rakhmatullina, Zashch. Metal 8, 230 (1972).
[9]M. H. Cohen and F. Reif, *Solid State Physics*, edited by F. Seitz and D. Turnbull (Academic, New York, 1957), Vol. 5.
[10]H. Abe, H. Yasuoka, and A. Hirai, J. Phys. Soc. Jpn. 21, 77a (1966).
[11]G. J. Perlow, C. E. Johnson, and W. Marshall, Phys. Rev. A 140, 875 (1965).
[12]R. M. Moon, Phys. Rev. A 136, 195 (1964).
[13]A. J. P. Meyer and G. Asch, J. Appl. Phys. 32, 3308 (1961).
[14]J. P. Rebuillat, IEEE Trans. Magn., 630 (Sept. 1972).
[15]A. J. Freeman and R. E. Watson, in *Magnetism* 2, edited by G. T. Rado and H. Suhl (Academic, New York, 1964).
[16]T. P. Das and M. Pomerantz, Phys. Rev. 123, 2070 (1961).
[17]K. W. Lodge and C. A. Sholl, J. Phys. F 4, 2073 (1974).
[18]K. C. Das, D. K. Ray, Phys. Rev. 187, 777 (1969).
[19]R. M. Sternheimer, Phys. Rev. 146, 140 (1966).
[20]R. E. Watson, A. C. Gossard and Y. Yafet, Phys. Rev. A 140, 375 (1965).
[21]L. Hodges and H. Ehrenreich, J. Appl. Phys. 39, 1280 (1968).
[22]J. M. Baker and F. I. B. Williams, Proc. R. Soc. A 267, 283 (1963).
[23](a) L. Evans, P. G. H. Sandars, and G. K. Woodgate, Proc. R. Soc. A 289, 108 (1965); (b) P. G. H. Sandars and J. Beck, *ibid.* 289, 97 (1965); (c) Y. Bordarier, B. K. Judd, and M. Klapisch, *ibid.* 298, 81 (1965).
[24]B. Bleaney, in *Hyperfine Interaction*, edited by A. J. Freeman and R. B. Frankel (Academic, New York, 1967).
[25]S. Ishida, J. Phys. Soc. Jpn. 33, 369 (1972).
[26]V. Zevin *et al.*, Phys. Rev. B 17, 355 (1978), following paper.
[27]P. Raghaven, E. N. Kaufmann, R. S. Raghavan, E. J. Analdo, and R. A. Naumann, Phys. Rev. B 13, 2835 (1976).
[28]F. W. De Watte, Phys. Rev. 123, 103 (1961).
[29]S. Muller, P. Bünner, and N. S. Pranghe, Z. Angew. Phys. 21, 403 (1967).
[30]H. B. G. Casimir, On the Interaction Between Atomic Nuclei and Electrons (Freeman, San Francisco, 1963).
[31]I. S. Mackenzie, M. A. H. McCausland, and A. R. Wagg, J. Phys. F 4, 315 (1974).